Controlled nanostructrures formation by ultra fast laser pulses for color marking

Benjamin Dusser, Sbigniew Sagan, Hervé Soder, Nicolas Faure, Jean-Philippe Colombier, Michel Jourlin, Eric Audouard

Controlled nanostructrures formation by ultra fast laser pulses for color marking

B. Dusser[1, 2, *], Z. Sagan[2], H. Soder[3], N. Faure[1], J.P. Colombier[1], M. Jourlin[1] and E. Audouard[1].

[1]*Université de Lyon, F-69003, Lyon, France, Université de Saint-Etienne, Laboratoire Hubert Curien (UMR 5516 CNRS), 42000 Saint Etienne, France.*
[2]*ATT (Advanced Track & Trace), 99 Rue de la Châtaigneraie Rueil-Malmaison, 92504 (France)*
[3]*Impulsion, Pôle Optique Vision, 18 Rue du Professeur Benoît Lauras.Saint-Etienne, 42000 (France)*
[*]*Corresponding author: benjamin.dusser@univ-st-etienne.fr*

Abstract: Precise nanostructuration of surface and the subsequent upgrades in material properties is a strong outcome of ultra fast laser irradiations. Material characteristics can be designed on mesoscopic scales, carrying new optical properties. We demonstrate in this work, the possibility of achieving material modifications using ultra short pulses, via polarization dependent structures generation, that can generate specific color patterns. These oriented nanostructures created on the metal surface, called ripples, are typically smaller than the laser wavelength and in the range of visible spectrum. In this way, a complex colorization process of the material, involving imprinting, calibration and reading, has been performed to associate *a priori* defined colors. This new method based on the control of the laser-driven nanostructure orientation allows cumulating high quantity of information in a minimal surface, proposing new applications for laser marking and new types of identifying codes

OCIS codes: (100.2000) Digital image processing; (100.2960) Image analysis ; (140.7090) Ultrafast lasers; (330.1710) Color, measurement

References and links

1. S.C. Tam, Y.M. Noor, L.E.N. Lim, S. Jana, L. J. Yang, M. W. S. Lau, C Y Yeo, “Marking of leadless chip carriers with a pulsed Nd:YAG laser,” Proceedings of the Institution of Mechanical Engineers. Part B. Journal of engineering manufacture, **207**, 179. (1993)
2. J. Qi, K.L. Wang and Y.M. Zhu, J. Mater, “A study on the laser marking process of stainless steel,” Journal of Materials Processing. Technology, **139**, 273. (2003)
3. M. Birnbaum, "Semiconductor Surface Damage Produced by Ruby Lasers," Journal of Applied Physics **36**, 3688-3689 (1965)
4. D. C. Emmony, R. P. Howson, L. J. Willis, "Laser mirror damage in germanium at 10.6 µm,"Appl. Phys. Lett., **23**, 598. (1973)
5. J. E. Sipe, J. F. Young, J. S. Preston, H. M. van Driel, "Laser-induced periodic surface structure. I. Theory," Phys. Rev. B, **27**, 1141. (1983)
6. J. F. Young, J. E. Sipe, H. M. van Driel, “Laser-induced periodic surface structure. III. Fluence regimes, the role of feedback, and details of the induced topography in germanium ,” Phys. Rev. B, **30**, 2001. (1984)
7. J.Reif, F Costache, M.Besthorn, in *Recent Advances in Laser Processing of Materials*, ed.(Elsevier, 2006), chap 9
8. A.J. Huis in’t Veld, J. van de Veer, “Initiation of femtosecond laser machined ripples in tseel observed by scanning helium ion microscopy (SHIM),” in *Proceeding on Laser Precision Microfabrication (LPM)*, Japan (2009)
9. Y. Shimotsuma, P. G. Kazansky, J. Qiu, K. Hirao, "Self-Organized Nanogratings in Glass Irradiated by Ultrashort Light Pulses," Phys. Rev. Lett., **91**, 247405. (2003)
10. A. Y. Vorobyev, Chunlei Guo, “Colorizing metals with femtosecond laser pulses,” Appl. Phys. Lett., **92**, 041914. (2008)

11. H. Lochbihler, “Colored images generated by metallic sub-wavelength gratings,” Optics Express 17,12189 (2009)
12. J. Wang, C. Guo, "Ultrafast dynamics of femtosecond laser-induced periodic surface pattern formation on metals,"Appl. Phys. Lett., **87**, 251914. (2005)
13. J. Wang, C. Guo, "Numerical study of ultrafast dynamics of femtosecond laser-induced periodic surface structure formation on noble metals," J. Appl. Phys., **102**, 053522. (2007)
14. M. Groenendijk and J. Meijer, “Microstructuring Using Femtosecond Pulsed Laser Ablation”, Journal of Laser Applications **18** (3), 227–234 (2006)
15. Z. Lin, L. V. Zhigilei, V. Celli, “Electron-phonon coupling and electron heat capacity of metals under conditions of strong electron-phonon nonequilibrium ,” Phys. Rev. B, **77**, 075133. (2008)
16. B. Huis in’t Veld, M. Groenendijk and H. Fischer, “On the Origin, Growth and Application of Ripples,” in *Proceedings of the 9th International Symposium on Laser Precision Microfabrication (LPM)* Quebec, Canada (2008)
17. M. Guillermin, F. Garrelie, N. Sanner, E. Audouard, H. Soder, “Single- and multi- pulse formation of surface structures under static femtosecond irradiation” Applied Surface. Science, **253**, 8075. (2007)
18. B. Dusser, E. Audouard, M. Jourlin, H. Soder, A. Foucou, “Method and device for marking a surface using controlled periodic nanostructures,” patent, WO/2009/090324. (2007)
19. A. R. Smith, “Color gamut transform pairs,” Computer Graphics, **12**, 12 (1978)
20. K.N. Plataniotis, A.N. Venetsanopoulos, in *Color Image Processing and Applications*, ed (Springer Verlag,2000)
21. J.P. Benzecri, « problème et méthode de la taxinomie, » Revue de statistique appliquée, 18, 73-78(1970)
22. J.P. Benzecri, in *La Taxinomie*, ed. (Dunot, 1973)
23. Johnson S., "Hierarchical clustering schemes", Psychometrika, **32**, 241-254 (1967)
24. N. Jardine, R. Sibson, in *Mathematical taxonomy* , ed. (Wiley, New-York, 1971)
25. Pavlidis T., "Hierarchies in structural pattern recognition", in *Proceeding of IEEE*, 67, (5), (1979), pp. 737-744
26. G. Dunn,B. Everitt, in *An introduction to Mathematical Taxonomy*, ed.(Cambridge University Press,1982)
27. J.P. Barthelemy, F. Brucker, "Binary Clustering,"Journal of. Discrete. Applied. Mathematics., **156**, 1237-1250. (2008)
28. P. Arbelaez, L. Cohen, " A metric approach to vector-valued image segmentation," International Journal of Computer. Vision, **69**, 119-126 (2006)
29. J.P. Benzecri, «Construction d'une classification ascendante hierarchique par la recherche en chaîne des voisins reciproques, » Les Cahiers de l'Analyse des Données., **7**, 209-218. (1982)
30. B. Dusser, Z. Sagan, A. Foucou, E. Audouard, M. Jourlin, “News applications in authentication and traceability using ultrafast laser marking” Proc. SPIE **7201**, 72010V. (2009)

1. Introduction

The ability to microstructure material surfaces, that is, to modify their micro- or nano-scale topographies, is important in several new technologies including optics, optoelectronics, mechanics, microfluidics, and permanent marking. Moreover, in a context of high precision processing of materials, variable information marking technologies are becoming more effective in marking industry [1,2]. Studying the interaction of lasers with surfaces reveals the formation of periodic structures produced by the laser beam when its power is close to damage threshold. In such interaction of intense light with materials, high excitation of solid surfaces results in nanostructure formation with size typically in the order of the wavelength, allowing a good spatial resolution. These structures, known to be strongly dependent of the characteristics of the incident electromagnetic field, have been widely studied in various cases of laser irradiation [3].

Nano-scale periodic structure formation under laser irradiation, so-called "laser-induced ripples", is commonly attributed to interference between the incident laser radiation and scattered or excited surface waves [4-6]. When ultra short laser pulses are used, the ripple structures consisting of mean spacing smaller than the wavelength of incident laser beam are called “fine ripples” and can no longer be accounted for by an interference mechanism only. In spite of a large number of papers on the subject of laser-induced periodic surface structures (LIPSS), the nature and the consequences of these waves in the formation of these structures remain unclear and have highly stimulated research in this field in recent years [7-9]. For ultra

fast irradiation regime, the usually observed periodicity is down to few hundreds of nanometers, and the structures are lightly but significantly material dependant, showing that it also depends on the matter response. Nevertheless the formed structures are always depending on beam properties such as laser polarization. The formation of these structures raises a fundamental question: how a structure induced by the incident electromagnetic field, whose duration is in the range of few hundreds of femtoseconds, can be "stored" in the matter since matter reaction occurs on picoseconds timescales. Many works are in progress to answer this question and it is not the goal of the present paper. The scope of the present work is to show how the obtained nanostructures with ultra short laser pulses can be precisely controlled, and used to obtain needed optical diffractive effects.

Color effect due to the diffraction of light by periodic structures on metallic surfaces has already been evidenced [10, 11]. Beyond these results, we demonstrate how to control such properties in order to transfer information on a metallic surface using this specific effect. Figure 1 shows an example of a color picture transferred on a metallic surface. The image is obtained with a usual reading scanner, and the present work focuses on giving details on the experimental procedure to obtain such results.

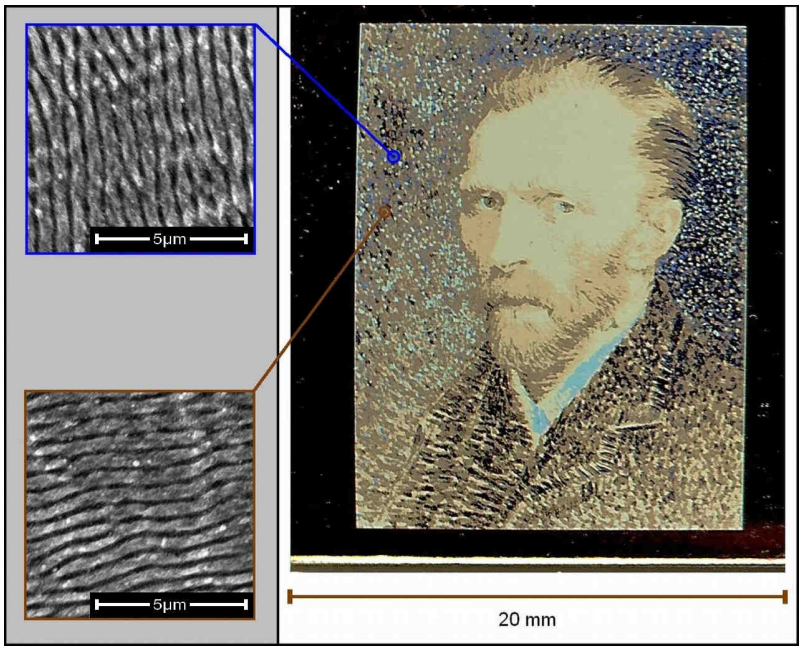

Fig. 1. On the right, example of color effects obtained by controlled nanostructures with a femtosecond laser chain on a 316L stainless steel sample, on the left, SEM X6000 images of controlled nanostructures marked with two different orientations.

2. Experimental section

2.1. Writing experimental set up

The laser system was a Ti:Sa laser chain which delivers 150 fs, 800 nm pulses at a repetition rate of 5 kHz. The total laser fluence range for marking stainless steel samples is from 0.2 J.cm-2 to 2.0 J.cm-2. The moving laser beam was focused with a F-Theta objective lens (f = 88 mm) or an achromat doublet lenses (f = 50.8 mm) (Figure 2). The beam diameter at the sample surface was in the range of 5 to 100 µm. The used sample is 316L stainless steel, a common industrial metal. Depending on the desired marking speed, two optical ways allow obtaining nanostructures (Figure 2); either by a motion of the sample itself or by the motion of

the laser beam. A large range of scan speed is available. As the laser pulse rate is fixed, the scan speeds correspond indeed in a variable overlapping of laser spots on the sample.

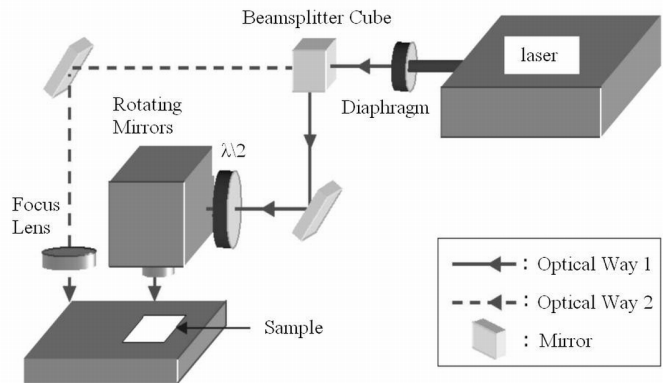

Fig. 2. Writing experimental set up with a femtosecond laser (2 W, 150 fs, 800 nm, 5 kHz). The figure show the two optical ways use in this article. The optical way 1 uses a rotating mirrors (HurrySCAN) with a F-Theta objective lens (f = 88 mm) and the optical way 2 uses an achromat doublet lenses (f = 50.8 mm).

2.2. Reading experimental set up.

We mention below a precise calibration of obtained colors has to be done, preferably with a simple and common tool for the flexibility of potential applications. Obviously the calibration procedure will be always dependant on the reading tool. We chose to use a very easy and wide spread tool: a scanner. With such a tool, color variations on the scanned picture of a marked material are due to the scanner's light diffraction on the nanostructures. The light emitted by the scanner is a white light, the wavelengths matching the different colors coming from a given ripples orientation can be found with the diffraction Equation (1):

$$m\lambda = d\left(\sin\alpha + \sin\beta\right) \tag{1}$$

With wavelength λ, groove spacing d, diffraction order m, incident light angle α and diffracted light angle β. As seen on Figure 3, the white light that was sent on the diffraction gratings constituted by the ripples which have a particular θ orientation to the axis of light. Through the light's optical path in the scanner, the different diffracted wavelengths resulting from the different orientations of the ripples are then integrated by the CCD sensor. If we add this orientation in the diffraction grating formula, we obtain the following Equation (2) :

$$m\lambda = d\left(\sin\alpha \cdot \cos\theta + \sin\beta\right) \tag{2}$$

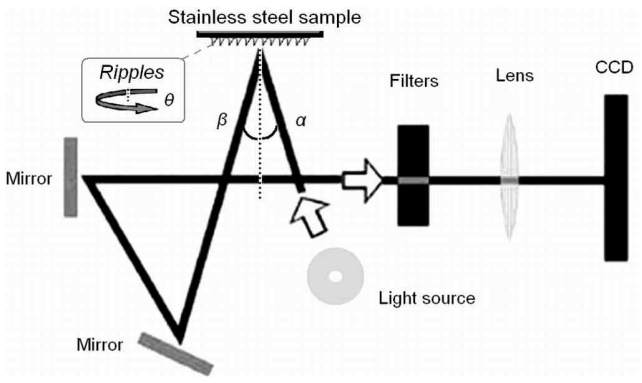

Fig. 3. Schematic Illustration of the light's optical path in a used scanner showed the principle of the reading procedure (see text).

3. Results and discussion

3.1 Ripples formation

The set up depicted in experimental section allows controlling several critical laser parameters: pulse energy, light polarization, spot size on the sample and overlapping of spots on the sample. When the target sample is moved perpendicularly to the incident laser beam, this overlapping can be varied from 0% (two successive spots are totally separated) to 100 % (two successive spots are totally super-imposed). To obtain a determinate energy density on the surface we can use either a high energy associated to a high speed or a low energy associated to a low speed. Results on surfaces are not identical, showing that each irradiation sequence is a specific way of matter excitation, determining the topography of the final state. The interaction process involves the energy deposition of the laser pulse and its transfer to the matter constitutive elements. Then, energy distribution and related effects are driven by the relaxation processes times. Depending on the intensity of the pulse, a local mesoscopic transformation occurs on a picosecond timescale, primarily due to a thermodynamic phase transformation. Consequently, nanostructures are mainly obtained for energy just near the ablation threshold, since laser irradiation transiently melts the surface before resolidification occurs. For higher fluences, the conditions of material ejection from the surface are reached, and ablation mechanisms prevent or reduce mechanisms of solid structure formation. Various examples of ripples aspect are shown in Figure 4, for beam power from 25 mW to 100 mW corresponding to pulse fluence from 0.4 J.cm-2 to 1.6 J.cm-2 and for each beam power, the obtained structures for scan speed from 10 mm.s-1 to 130 mm.s-1.

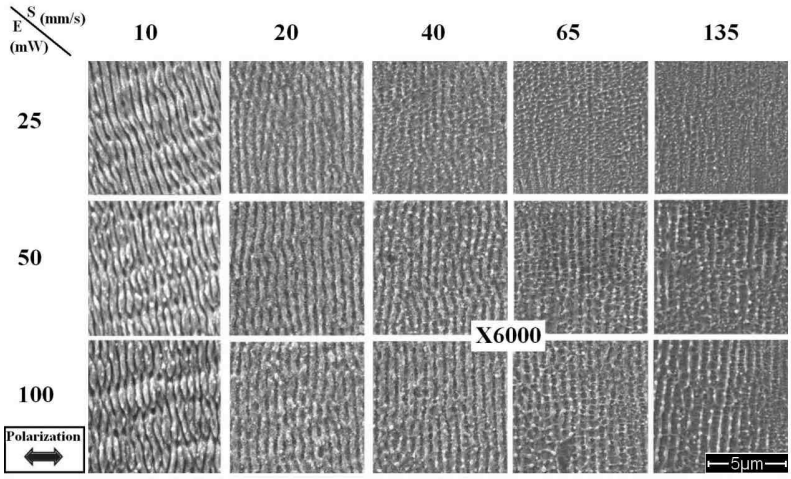

Fig. 4. SEM X6000 images of ripples obtained with the "optical way 2" femtosecond laser chain (150 fs, 800 nm, 5 kHz, achromat doublet lenses: f = 50.8 mm) on stainless steel 316L. The different ripples aspects are obtained with a beam power from 25 mW to 100 mW (fluence from 0.4 J.cm-2 to 1.6 J.cm-2) for rotating mirrors speed from 20 mm.s-1 to 130 mm.s-1.

As shown on the Figure 4, clarity of contour and edges of the quasi-linear structures are typically obtained for stainless steel, which is a widely used metal for industrial applications. Reproducible sub-wavelength ripples are presented on the Figure 4, showing particularly the main structures used for this work, above called "fine" ripples. Their spacing is typically 660 nm and they are 200 nm high. The speed and energy range in which the ripples shape is conserved, provide a typical windows of working parameters (Figure 4). Indeed the dependence of the ripple spacing and magnitude on the materials properties is hardly

predictable. The driving force structuring the liquid and the characteristic time needed to transfer these structures into the solid phase upon solidification appears to be connected to material properties such as electron-phonon coupling, thermal conductivity or surface tension [12-14]. To explain the difference in the observed surface ripples among the different metals, the dynamic processes following laser excitation in metals have to be considered. Solid structure formation results from a complex interplay between various mechanisms and each process depends on specific material characteristics and transport properties which are not accurately known for alloys in this ultra fast regime. Consequently, ripples formed on alloy surfaces can be hardly discussed, since relaxation dynamics depend on the properties of differing individual components. But experimental evidence shows that interaction and relaxation processes, in the case of stainless steel, lead to a sharp ripples formation.

Irradiating a metal by a sufficiently short laser pulse can lead to a significant temperature rise of the electrons with respect to the ionic lattice. A new thermal equilibrium will be reached later, after several picoseconds, when collisions between excited electrons and phonons have transferred energy among them. Thus thermal transport properties and particularly the electron-phonon coupling factor is a fundamental parameter leading the relaxation process. Assuming that Stainless Steel has properties similar to Iron one's, stainless steel is supposed to have an electron-phonon coupling factor very high at room temperature (20 times Aluminium, 200 times Gold) [15]. Electron-phonon coupling strength determined the balance between energy coupling and hot electron diffusion, following femtosecond laser excitation. The competition of these two ultra fast dynamic processes may determine the clearness level of periodic surface patterns and the strong value of its parameter make stainless steel a good candidate for surface structuration. Other types of structures can be observed, the commonly observed ones, which spacing is linked to the wavelength (800 nm) as the formation mechanism is a surface interference one [7]. We will call them "coarse" ripples (Figure 4, V = 10 mm.s-1 and E = 100 mW). Furthermore, we can also put in evidence a third kind of ripples, which can be seen in previous shown results (Figure 4, V = 130 mm.s-1). Their spacing is lower (150 nm) and they are typically perpendicular to the fine ripples, they have thus the same orientation as the coarse one. These "ultra fine" ripples are only scarcely reported in the literature [16], and they may bring complementary observations to the effort of understanding ripples formation.

In the present work, neither coarse ripples, nor ultra fine ones have a significant influence to diffractive effects studied below, because of their non adapted spacing regarded to the standard reading light used. To evidence this diffractive effect in the best conditions, the experimental parameters have to be chosen in order to promote fine ripples formation. In the following, we will explore in more details these optimized conditions of fine ripples formation.

We will thus investigate the experimental conditions to obtain optimized ripples on surface in order to use them for marking applications. One has to point out two characteristics useful for these applications:

- Ripples can be obtained on a wide surface with only a slight overlapping of pulses

- Ripples can be obtained with a single-pulse exposure [17].

Of course these two characteristics are the conditions to a systematic and industrial use since it is the key factor for a high speed technology in a field of marking where high productivity is a go/no go breaking point.

With the presented writing set up, two technical ways are possible to obtain ripples on a surface with a determinate scanning speed. This scanning speed is obtained either by moving the sample thanks to motion stages or by moving the beam thanks to the rotating mirrors. In Figure 5 we show that both ways produce nearly the same structures if the corresponding speeds are the same.

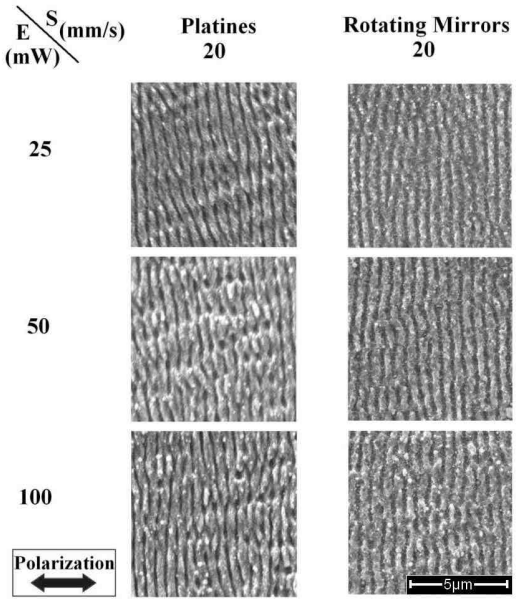

Fig. 5. SEM X6000 images of ripples obtained with a femtosecond laser chain (150 fs, 800 nm, 5 kHz, rotating mirrors) on stainless steel (316L). The different ripples aspects are obtained with a beam power from 25 to 100 mW (fluence from 0.4 J.cm-2 to 1.6 J.cm-2) with a 20mm.s-1 rotating mirrors speed. On the left, the ripples are obtained with the "optical way 2" (achromat doublet lenses: f = 50.8mm) and on the right, the ripples are obtained with the "optical way 1" (rotating mirrors, F-Theta lens: f = 88mm).

Mechanical motion stages provide accuracy, repeatability and a fine resolution for low speed process whereas the rotating mirrors allows a large process tool with a high speed. Notice the case, mentioned above, of low speed (high energy density) where "coarse" ripples appear.

An important parameter is the overlapping rate, i.e. the number of pulses superimposed on the same area and settled by the scanning speed. This number of pulses is mentioned in Figure 5, but ripples can be also obtained without overlapping, the pulses are thus next one to the other, and their number are settled by the laser control unit, as illustrated in Figure 6. The point by point method can be thus used for marking.

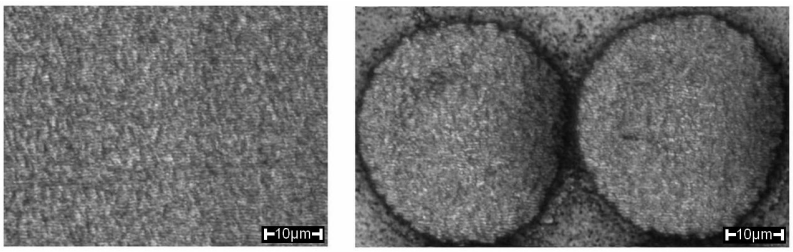

Fig. 6. Optical microscope image X2000 of ripples obtained with the "optical way 2" femtosecond laser chain (25 mW, 0.4 J.cm-2, 150 fs, 800 nm, 5 kHz, achromat doublet lenses: f = 50.8 mm). The overlapping process is use on the left, and the point by point process is used on the right.

Ripples structures are quite similar in both cases. In the point by point case, we observe areas without ripples due to the circular shape of the spot. This could affect the contrast in the reading procedure presented below but the effect is not noticeable.

The main point, concerning ripples formation to achieve marking applications, is the ability to control ripples direction thanks to laser polarization. This can be clearly seen in Figure 7 where polarization has been tilted in three particular angles.

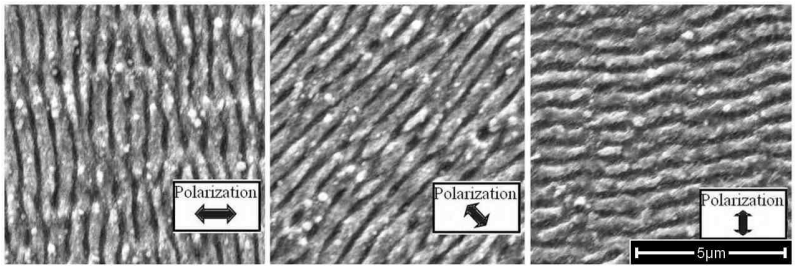

Fig. 7. SEM image X6000 of ripples obtained with the "optical way 2" femtosecond laser chain (P = 100 mW, F = 1.6 J.cm-2, rotating mirrors speed = 20 mm.s-1) on stainless steel 316L. On the left, ripples marked with a 0° polarization angle. In middle, ripples marked with a 45° polarization angle. On the right, ripples marked with a 90° polarization angle.

As mentioned above, the physical reasons of the dependence between laser polarization and ripples orientation remains unclear but the control of ripples orientation can be very precise. The sensibility of the method can be measured leading to a precise calibration of ripples direction with laser polarization. With the best reachable precision, a difference of $\Delta\theta$ in laser polarization leads to a change of $2\Delta\theta$ in ripples direction. In the following, this resolution will be studied not in terms of ripples direction, but in terms of induced color effect change, as it is the specificity of the presented work.

3.1. Color effect reading:

The phenomenon used to read nanostructures is simply light diffraction. The patented specific technique we use is to read very precisely the nanostructures orientation [18], based on the diffractive effect, when these nanostructures are exposed to a non coherent light. It is thus a "macroscopic reading", not based on structural and dimensional analysis as seen earlier. Optical ripples properties are indeed close to those of diffraction gratings. It is therefore possible to identify those ripples through this induced diffraction phenomenon, i.e. a color effect obtained by light illumination of "rippeled" surface. This effect has already been reported but had never been used for color calibration. Indeed, A. Y. Vorobyev and C. Guo have already investigated on this colorized effect on rippled metal surfaces but these authors have not proposed the control of this color effect by the ripples orientation with a suited calibration [10]. H. Lochbihler has shown the potential obtaining of images on metallic surfaces with nanostructures but with writing procedure using classic gratings engraving [11]. Of course gratings obtained by standard methods are of better quality in terms of surface pattern, but the results in terms of color spectrum are not wider than the results presented below, obtained with ripples which appear easily on metallic surfaces as shown before.

In practice, two experimental methods, discussed in experimental section, have been used to mark samples. One is point by point marking and the second one is spot overlapping process marking. In the following, we will use the point by point method in the presented examples. Figure 8 shows examples of a colorimetric variation depending on laser marking parameters such as pulses number. In the present case, a range of 10 to 50 pulses per pixel appears to be optimal to obtain a good contrast of colors.

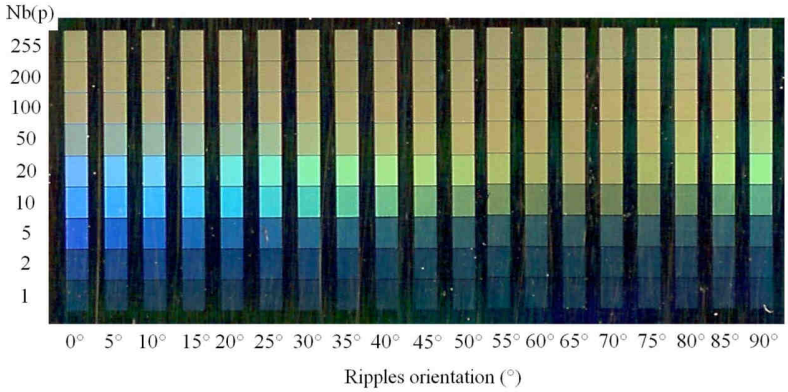

Fig. 8. Scanned image (1200 dpi) of stainless steal sample (316L) marked by 9 lines of nineteen squares obtained with the "optical way 1" femtosecond laser chain (P = 25 mW, F = 0.4 J.cm-2). Each line uses a "point by point" marking method and each square has been marked with different ripples orientations (from 0° to 90°). Each point of the scroll up lines has been marked with different numbers of laser pulses (from 1 laser pulse/point on the bottom line to 255 laser pulses/point on the top line).

A crucial question arises concerning the use of the ripples colored effects: how much colors may be obtained with a high reliability level, allowing their reading by an image acquisition system. Our approach to solve this problem consists in marking the pixel of a sample with a small variation of ripples orientation (10° for example in Figure 9).

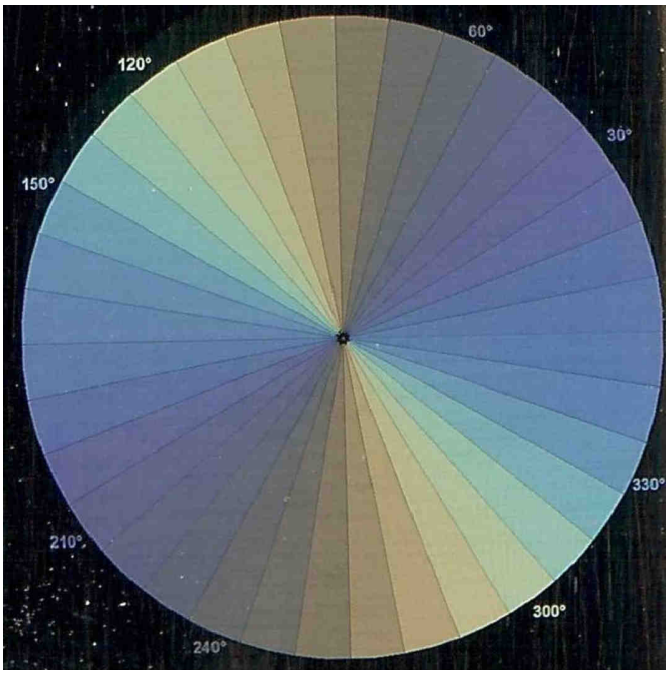

Fig. 9. Scanned image (1200 dpi) of stainless steel sample (316L) marked by thirty six discs section obtained with the "optical way 1" femtosecond laser chain (P = 25 mW, F = 0.4 J.cm-2). Each section have been marked with different ripples orientations (from 0° to 350°).

In this way, we obtained curves (Figure 10) in the HSV (Hue, Saturation, Value) color space [19], representing the color components variations in relation with the ripples orientation.

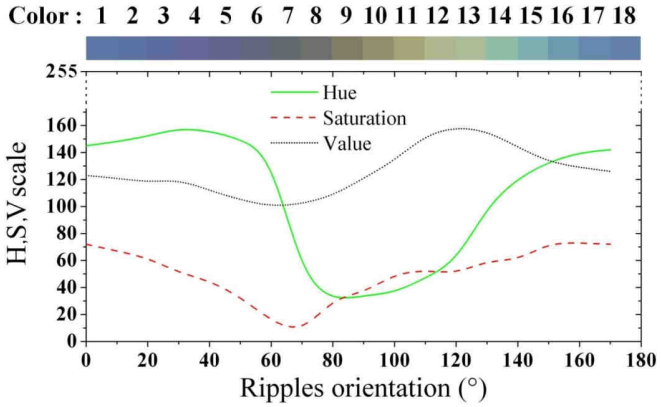

Fig. 10. Evolution of HSV (Hue, Saturation, Value) components perceived by the scanner acquisition of different colors obtained by ripples laser marking depending on ripples orientation.

HSV is a nonlinear transformation of the classical RGB color space. The main advantages of the HSV color space over RGB color space are [20]:

- Good compatibility with human's colors perception.

- Color can be named and chosen by first picking one axis: the hue axis (green curve in Figure 10), instead of 3 axis for the RGB color space.

A first observation of these curves shows that the slope at each curve varies differently and erratically. Indeed these slopes at each HSV curve are more or less important at different ripples orientation and can be explained by the fact that colors variations are not linear. As we know, most of classification algorithms (ex : k-mean, isodata...) necessitate an a priori knowledge of the desired classes number, we decided then to apply an image classification technique able to determine the number of efficient accessible colors.

In order to determine the optimal number of color classes, we decided to use the "Ascendant Hierarchical Classification" (AHC) method [21-26]. This method which is a powerful approach in data analysis, is also used in image segmentation. For these applications in image processing, the AHC does not present difficulty and offers two important advantages:

1-The method does not require an a priori knowledge on the classes number: on the opposite, it provides the “hierarchy” of all the intermediate classifications of the image, from the low level where each single color corresponds to a class, to the ripples level where all the colors are placed into a unique class.

2- In order to perform the color grouping, we must choose a “distance” between colors. At the beginning of the AHC algorithm, the classes number corresponds to the number of different colors. Two colors are considered as different if their distance is strictly positive: this constitutes the hierarchy lowest level. At the following level, we aggregate the two colors whose distance is the smallest and these two colors lie now in the same class. This technique, which consists in grouping the nearest colors, is then performed until all the colors are considered in the same class (hierarchy highest level). At each step of the classification, we associate an information which is the “tolerance” from the precedent step to the current one.

Such information permits to put in evidence the most significant steps which correspond to the largest tolerances and then appears as a “confidence” measurement associated to each level of the AHC. We use in the following either 6 or 9 colors of 18 available (Figure 11). It is clear that a lot of other ways of classification exist [27, 28], but our aim here is not to compare various color metrics.

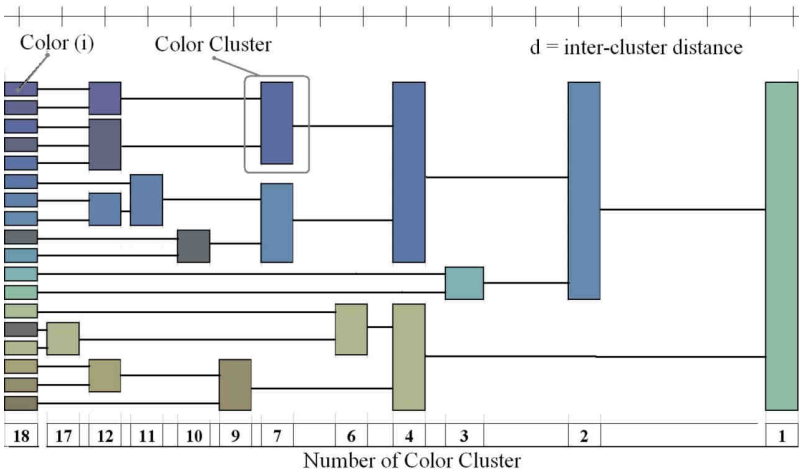

Fig. 11. Example of Ascendant Hierarchic Classification dendrogram obtained with ripples color (i) marking process (eighteen ripples orientations).

4. Color printing process by oriented nanostructures

We illustrate our new marking method by the duplication of a picture using the colors created with our method and based on the established principle: one ripple's orientation equals one color. On a chosen image, we determine the number of main colors. We associate these colors with color classes available with this laser marking process. To do this, we simply distribute each pixel of the original image in one of the available color classes. This can be achieved for example in the classical HSV color space

We calculate the distance between each pixel of the initial image to each class of color, and we combine the value of pixel color in the table to the closest class of color. Different distances can be used successfully for this marking process [29]. The distances used here is the unweighted pair-group average linkage. It has automatically reduced the number of colors of the image to the number of color classes available by the marking and viewable by the scanner. Once this is done, we create the color planes corresponding to the ripples orientations to engrave. These planes represent what the laser must mark on the metal sample for each ripples direction associated with the expected color. A simulation of obtained image can be computed and compared with final sample of stainless steel read with the scanner. (Figure 12) illustrates all these steps. The total time for writing the image presented in Figure 12 is typically 3 minutes. Of course this time depends on several laser parameters (number of pulses, repetition rate…), the size of the image, the number of color planes and pixels to engrave. Optimizing these parameters is not the scope of this present work, but this time process can be reduced easily by a factor 10.

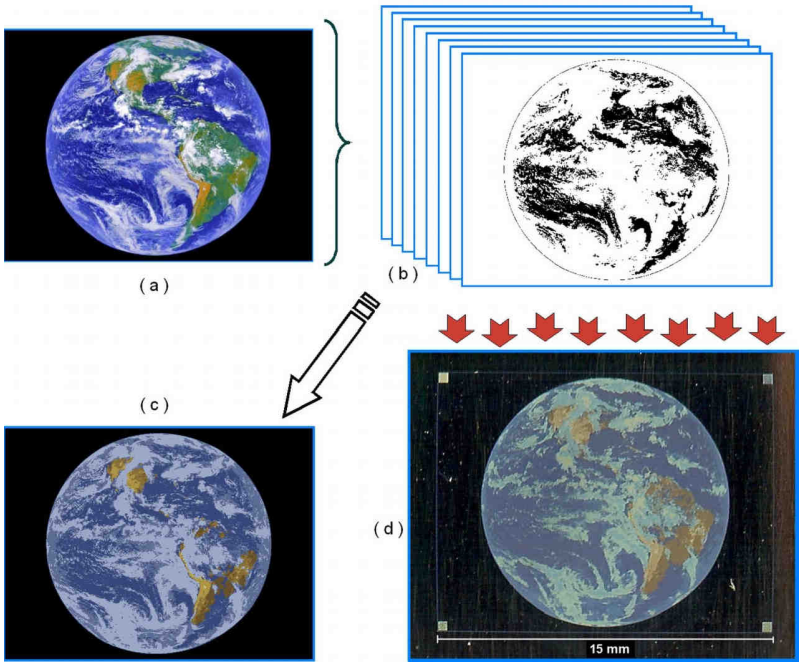

Fig. 12. Segmentation by image processing into height laser marking planes (b) of an initial image (a) and computer simulation of the expected color marking result (c). Scanner image (1200 dpi) of stainless steal sample (316L) marked with height planes of ripples (d). Each plane is marked with his own ripples orientation.

5. Conclusion

Through the centuries painters have constantly innovated by creating their own colors mixes on many types of surface. Even high technologies allow exploring original painting techniques, inspired by impressionism approach, using a laser source. Nanostructures generated by ultra short pulses produce colored shapes on a metal surface by diffraction process, and can be designed as the colors of a painter. Composed of nanostructures, with a user defined orientation associated with laser polarization, the assembly allows returning a pre-defined picture thanks to a suitable colorimetric calibration. A complete method, from marking to reading, and including perceptual color relationships has been proposed to impress information or data on the metal surface. Obviously, painting is not the purpose of this work, which opens the way to authentification and traceability of a product [30]. In these fields, many innovative marking processes can be proposed. For instance, in the case of 2D classical code, like datamatrix, each pixel can be marked using nanostructures with controlled orientations. A third information axis or more can be thus created. Compared to classical existing tools, the advantages are important: high difficulty of copying, ability of containing much more information in a marking reduced in size and also an easy reading procedure. On the opposite, marking using ultra short pulses has to overcome typical steps of new technologies in industry, particularly the high level of investment. Concerning this point, it has to be pointed out that the nanostructures formation presented here is a non ablative mechanism, and the laser energy needed can correspond to non amplified laser systems. An ultra fast oscillator, cheaper and with high repetition rate, is thus a good candidate for applications of high productivity.